Magnetic Dipole and Higher Pole Interaction on a Square Lattice

Melanie Ewerlin,[1] Derya Demirbas,[1] Frank Brüssing,[1] Oleg Petracic,[1,*] Ahmet A. Ünal,[2] Sergio Valencia,[2] Florian Kronast,[2] and Hartmut Zabel[1]

[1]*Institut für Experimentalphysik/Festkörperphysik, Fakultät für Physik and Astronomie, Ruhr-Universität Bochum, Bochum 44780, Germany*

[2]*Helmholtz Zentrum Berlin, Elektronenspeicherring BESSY II Albert-Einstein-Strasse 15, Berlin 12489, Germany*

(Received 28 December 2012; published 26 April 2013)

We have studied the magnetic interaction of circular magnetic islands with a dipole character on a square lattice. The square pattern consists of lithographically prepared polycrystalline PdFe islands, 150 nm in diameter and a periodicity of 300 nm. Below the Curie temperature at 260 K, the islands are in a single domain state with isotropic in-plane magnetization. Below 160 K, there is an onset of interisland interaction that leads to a change of the shape of the hysteresis, an increase of coercivity, and a development of in-plane anisotropy. Photoemission electron microscopy with circularly polarized incident x rays tuned to the L_3 edge of Fe confirms the increasing correlation of the magnetic islands and the formation of elongated chains, as predicted by Vedmedenko *et al.* [Phys. Rev. Lett. **95**, 207202 (2005)] for contributions from pole interactions of higher order than the dipolar one. Neighboring chains are found to be irregularly oriented either parallel or antiparallel.

DOI: 10.1103/PhysRevLett.110.177209 PACS numbers: 75.75.−c, 75.10.−b, 75.70.Ak

Fluctuations, orderings, and phase transitions of magnetic dipoles on a two-dimensional square lattice remain an interesting and challenging problem in statistical physics. Although theory predicts a noncollinear antiferromagnetic ground state for a square lattice [1], the exact nature depends on details of the interaction and boundary conditions [2–7]. Pointlike magnetic dipoles are only available in the form of condensed atoms. But usually the interaction is too weak for forming an ordered ground state. To remedy this problem, extended single-domain magnetic islands can artificially be fabricated carrying a macrospin with sufficiently high magnetic stray fields. However, these islands cannot solely be considered as pure magnetic dipoles. Instead, higher pole interactions need to be taken into account [2,8]. While each individual dipole can be designed as to display a continuous in-plane symmetry with essentially zero coercivity, turning on dipolar interactions creates for itself an effective anisotropy and increases the coercivity [5,6]. While lithographic methods permit fabrication of magnetic materials into square lattices decorated by circular islands [9–11], experimental verification of their phase transitions and concomitant ground states are missing so far.

The expected scenario of the sequence of phase transitions from high to low temperatures can be described as follows, starting with an array of paramagnetic circular islands placed in close proximity on a square lattice [see Fig. 1 (left panel)]. Each individual island has a critical temperature T_{C1}, which is determined by the local exchange interaction and the finiteness of the island. Below T_{C1} the islands enter a ferromagnetic single-domain state with a dominant dipolar character but without any in-plane anisotropy of the individual dots. Because of the low magnetization, the dipolar stray fields are weak and thermal fluctuations overcome *interisland* ordering. In this temperature regime the islands form a superferromagnetic state [12], while the *intraisland* order is ferromagnetic [Fig. 1 (middle panel)]. As the temperature is lowered further, the magnetization increases and so does the dipolar field of all islands.

For $k_B T_{C2} \leq E_{\text{dipole}}$, where

$$E_{\text{dipole}} = \frac{\mu_0}{8\pi} \sum_{i,j(i\neq j)} \frac{1}{|\mathbf{r}_{i,j}|^3} [(\mathbf{m}_i \cdot \mathbf{m}_j) - \frac{3}{|\mathbf{r}_{i,j}|^2} (\mathbf{m}_i \cdot \mathbf{r}_{i,j})(\mathbf{m}_j \cdot \mathbf{r}_{i,j})], \quad (1)$$

with $\mathbf{m}_i$ and $\mathbf{m}_j$ the magnetic moments of two islands and $\mathbf{r}_{i,j}$ the distance vector between the centers of the islands, the dipolar interaction becomes sufficiently strong as to cause

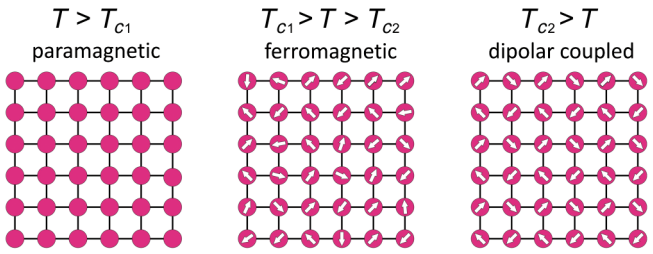

FIG. 1 (color online). Schematics of phase transitions in a magnetic nanodot array. Left: Above T_{C1} the islands are in a paramagnetic state. Middle: For $T_{C1} > T > T_{C2}$ the islands are in a single-domain ferromagnetic state and act predominately as magnetic dipoles without long range order. Right: For $T_{C2} > T$ the dipolar stray fields of the individual islands are sufficiently strong as to cause a dipolar ordering determined by the symmetry of the pattern.

long range order. The two phase transitions are decoupled, since the exchange interaction is local and limited to the island size, whereas the magnetic dipole interaction is long range. The main question is the following: what is the ground state that results from both interactions below T_{C2}? This is what we try to answer in this Letter.

Theory and Monte Carlo simulations predict that in the case of freely rotating dipoles on a square lattice, several degenerate ground states can be realized. Two sublattices A and B may, for instance, be arranged in a noncollinear antiferromagnetic order as depicted in Fig. 1 (right panel) [1,7,13]. For finite arrays with real dipolar particles, higher pole interactions need to be taken into account. In this case, theory predicts an increasing anisotropy, an opening of the magnetic hysteresis, and a ground state that consists of chains of interacting dipoles arranged parallel or antiparallel, forming irregular domains [2].

The scenario which we discuss here should be distinguished from free dipoles on a triangular lattice, where the ground state is a vortex state [14]. It should also be distinguished from square spin ice patterns, where magnetic dipoles are fixed in position but are allowed to flip their orientation [15–18]. In our present case, the aim is to design a magnetic dipole array where the anisotropy is solely introduced by interaction, not by shape.

In order to study a system as outlined above we need a material which provides experimental access to both transition temperatures T_{C1} and T_{C2}. It should have a Curie temperature close to room temperature, be magnetically very soft, and with negligible magnetic anisotropy. A material which fulfills these requirements is a $Pd_{1-x}F_{ex}$ alloy. The Curie temperature scales roughly linearly with the Fe concentration [19,20]. For the present experiments we have chosen an Fe concentration of 13 at. %, resulting in a Curie temperature of 290 K [21]. A system with such a critical temperature has the additional advantage that it can be reset easily by temperature cycling above T_{C1}. The choice of a higher Fe concentration for enhanced interaction is prohibited because of an increasing tendency for perpendicular anisotropy [21–23].

$Pd_{0.87}Fe_{0.13}$ films were prepared by ion beam sputtering at room temperature on a Si substrate with a 1.5 nm thick Ta buffer layer for reducing the roughness and enhancing the adhesion of the PdFe film. This procedure generates polycrystalline films, which eliminates effectively any magnetic anisotropy in case there was one remaining. Finally, all samples were capped with a 5 nm Al_2O_3 layer for oxidation protection. The roughness of the films was on the order of 0.3 nm as determined by atomic force microscopy.

The magnetic characterization of the PdFe film was performed using a superconducting quantum interference device and a low temperature azimuthally dependent longitudinal magneto-optic Kerr effect (MOKE). From the magnetization $M(T)$ of the continuous film, a Curie temperature of 290 K is estimated. Magnetic hysteresis curves taken at 80 K confirm the soft magnetic character of the $Pd_{0.87}Fe_{0.13}$ alloy film with a coercive field of only 2.3 Oe, an in-plane easy axis, and no azimuthal magnetic anisotropy.

Before patterning the alloy film into a square lattice of circular islands, we have performed micromagnetic simulations of the expected magnetic ground state of an individual dot as a function of diameter d and thickness b, using the OOMMF package [24]. The resulting phase diagram shows two states: a vortex state for bigger islands and a single-domain state for smaller islands. For the fabrication of magnetic islands we have chosen parameters which lie safely in the parameter space where a single-domain state is expected. Those require a diameter of $d = 150$ nm and a thickness of $b = 10$ nm. Nanostructuring was performed by electron beam lithography [17]. After e-beam exposure and the developing of a negative photo resist, the structures were transferred into the metallic layer by ion beam etching. The dots are arranged on a square lattice with a periodicity of 300×300 nm^2. Each writing field has a lateral size of 50×50 μm^2 and 15×15 writing fields are placed on one sample. Figure 2 shows a scanning electron microscope image of the nanostructured and etched sample. This image confirms the circular shape of the islands required for an isotropic in-plane anisotropy and a highly regular square pattern.

Each individual island contains about 10^6 Fe atoms. Assuming a local magnetic moment of 2.2 μ_{Bohr} for Fe as in bulk Fe, the total moment of each island is on the order of 2×10^6 μ_{Bohr}. From this we estimate within the dipole approximation a magnetic field of 740 Oe which one island exerts on the other at a distance of 300 nm and at a temperature $T = 0$ K. As the dipole field scales with the magnetization, it will be much weaker just below T_{C1}, but at $T_{C2} < T_{C1}$ the dipole field will be sufficiently strong to induce order.

For exploring the magnetic properties and the phase diagram of the circular dot pattern, magnetic hysteresis measurements are most useful. However, because of the dilute magnetic alloy and the small total amount of

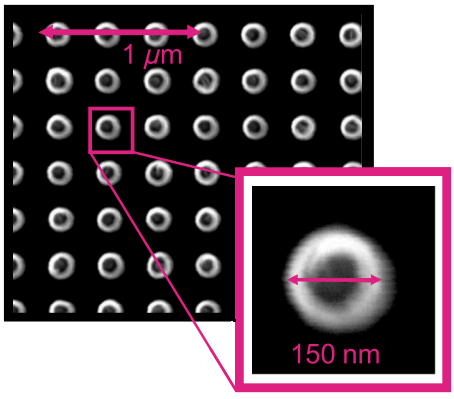

FIG. 2 (color online). Scanning electron microscopy image of a PdFe dot array placed on a 300×300 nm^2 square lattice by e-beam lithographic means. The zoomed in dot shows the shape and a diameter of 150 nm. The white rim is due to edge effects and residual resist.

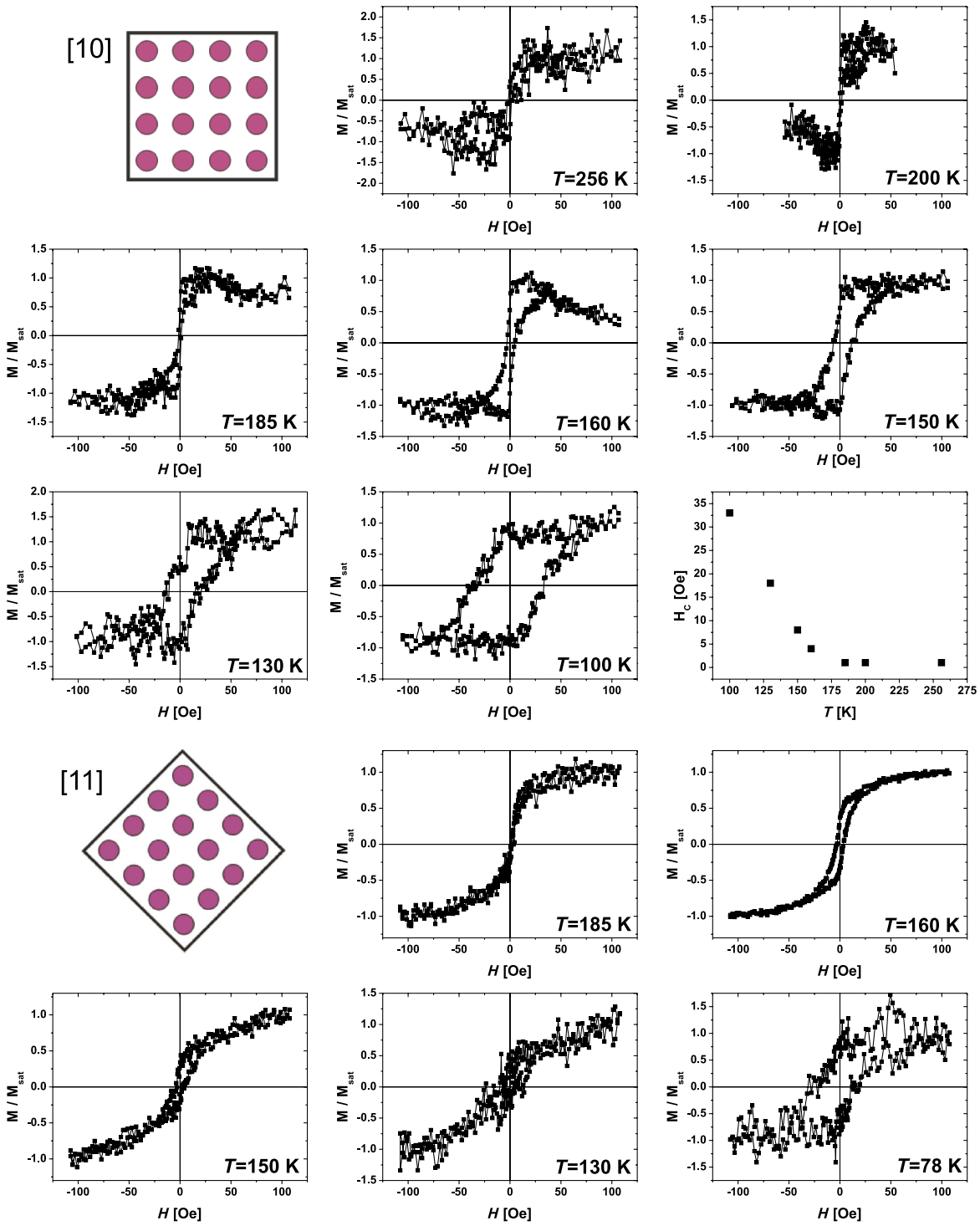

FIG. 3 (color online). Hysteresis measurements recorded with the magneto-optic Kerr effect in longitudinal configuration for different temperatures. The top 3 rows reproduce the hysteresis loops for the [10] orientation of the dot array. In the last panel of this sequence the coercive field is plotted as a function of temperature. The bottom two rows show the hysteresis for the [11] orientation, i.e., after rotation by 45°. All hysteresis curves are normalized by the saturation value. Note that the range on the y axis varies according to the noise level in saturation.

magnetic material, neither a superconducting quantum interference device nor resonant magnetic soft x-ray scattering turned out to be sensitive enough to resolve a magnetic hysteresis with acceptable statistics. Therefore we performed low temperature MOKE measurements in the longitudinal configuration using Helmholtz coils to avoid residual fields at remanence and to compensate the earth magnetic field. Hysteresis loops were taken in a range from

room temperature down to 80 K and were averaged over about 260 field cycles. The results of the hysteresis curves are shown in Fig. 3 for the [10] and [11] orientations of the pattern.

At $T = 256$ K we notice an onset of a ferromagnetic state, a clear hysteresis becomes visible with a very small coercivity of about 1 Oe. We take this as an indication for an onset of an intraisland ferromagnetic state with negligible interisland dipole interaction. The onset temperature T_{C1} is lower than the critical temperature T_c of the continuous film, which is to be expected due to finite size scaling. At lower temperatures the shape of the hysteresis curves changes drastically. At 185 K the hysteresis curve opens up before reaching saturation while the coercivity remains small. This is even more pronounced at 160 K and is usually a sign for some *s*- or *c*-type buckling spin state within the islands [25,26]. Below 160 K the shape of the hysteresis changes again significantly. In the [10] orientation the shape of the hysteresis resembles a parallelogram with increasing coercivity of up to 33 Oe at 100 K and a 100% remanence. The coercivity versus temperature is plotted in Fig. 3, the last panel of the third row. The increasing coercivity and the slanting of the hysteresis with decreasing temperature is indicative for an increasing interisland interaction with decreasing temperature below 160 K. In contrast, the hysteresis loops in [11] orientation show low remanence and a high saturation field, which is typical for a hard axis behavior. Thus, at low temperatures the PdFe-nanodot array clearly develops features of magnetic anisotropy. The anisotropy in addition to the increasing coercivity are strong indications for interisland pole interaction with contributions of higher order than the dipolar one.

To confirm the interisland interaction and possible ordering of the square magnetic dot array below 160 K we have performed magnetic imaging experiments using magnetically sensitive x-ray photoemission electron microscopy (X-PEEM) at the BESSY II of the Helmholtz-Zentrum Berlin [27]. X-PEEM measurements were performed at various temperatures below T_{c1} in magnetic remanence. Images were taken with right (σ^+) and left (σ^-) circular polarized incident *x* rays tuned to the resonant energy of the Fe L_3 edge. Magnetic contrast is achieved by evaluating the so-called magnetic asymmetry, i.e., $A = (\sigma^+ - \sigma^-)/(\sigma^+ + \sigma^-)$. In Fig. 4 the asymmetry is plotted, where the colors encode the orientation of the in-plane magnetization as indicated by arrows in the top panel. The rows of islands are aligned parallel to the incident light propagation direction, where the magnetic asymmetry, hence, the magnetic contrast, is largest. It is important to note that the images show the ground state of the sample after cooling down from the paramagnetic state without applying any magnetic field. Above 220 K no magnetic asymmetry is observed. At 180 K some dots attain a magnetic contrast, but without any discernable correlation. At $T = 160$ K the dots clearly show magnetic contrast and start to become correlated in the form of chains, as seen in the image Fig. 4 (top panel). At the lower temperature of 140 K [Fig. 4 (bottom panel)], the magnetization of the individual dots has increased, as seen by an increase in the contrast of the asymmetry images. Moreover, the number of dots with a large magnetization pointing either parallel or antiparallel to the incoming beam direction has increased dramatically and they form chains. These chains are preferably oriented parallel to the [10] and [01] perpendicular lattice directions, the latter ones appear white because of a lack of contrast in the perpendicular direction. The chain length is observed to increase with a decreasing temperature (see inset in the top panel of Fig. 4) as a result of an increasing dipolar interaction. Very few dots exhibit two colors. We take this as an indication for thermal fluctuations of the magnetization orientation in the stray field of a neighboring island during the integration time of about one hour. Deflections of the

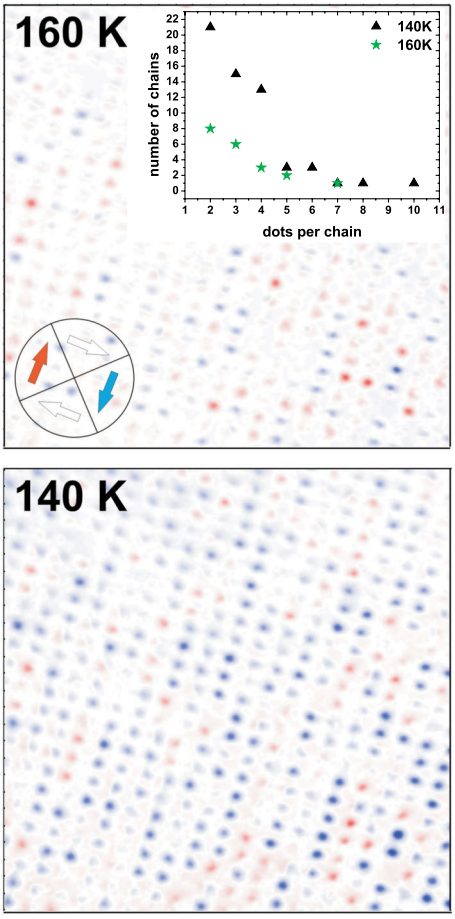

FIG. 4 (color online). Space resolved images of the magnetization of PdFe islands taken with polarized photoemission electron microscopy using right and left circular polarized synchrotron radiation tuned to the L_3 edge of Fe. Shown is the asymmetry of the images for different temperatures. The orientational dependence of the magnetic sensitivity is color coded according to the color circle shown in the inset. The inset in the top panel shows the number of dots per chain for different temperatures.

electron yield of those particular dots by local field fluctuations result in a slightly broadened two color image. In the scanned area the frequency of blue chains is highest. This changes for different areas scanned and also after repeated cooling cycles. The predominance of one color, i.e., one particular domain, is a sign for higher pole interacting islands.

For pure dipole-dipole interaction, theory predicts a canted antiferromagnetic state as shown schematically in the right panel of Fig. 1 [2,3,5–7]. Translated into PEEM contrast, the canted antiferromagnetic state would manifest itself in a regular pattern of antiparallel red and blue chains. However, here we observe an ordering in form of parallel blue chains interrupted by red chains without forming a regular pattern. This type of ordering is completely supported by theory, if in addition to the dipole-dipole interaction, higher pole interactions are also taken into account [2]. Furthermore, in the case of pure dipolar interaction on a square lattice, the magnetization versus the applied field should not show any appreciable hysteresis. But for dipole plus higher pole interaction, a real hysteresis with a finite coercivity and increasing squareness is expected. The simulated hysteresis by Vedmedenko *et al.* agrees very well in shape with our experimental MOKE results for the easy axis [2]. In particular, the parallelogram-like shape is very well reproduced. According to Vedmedenko *et al.* it is mainly the octopolar term which is responsible for the antiparallel but irregular chain formation and for the opening of the magnetic hysteresis. Although magnetic interaction on square dot arrays was studied in the past [28], the detailed features of chain formation, elongation, and development of hysteretic behavior with increasing coercivity and squareness with decreasing temperature is seen here for the first time.

In conclusion, by combining MOKE and PEEM experiments, we have shown that on a square lattice decorated with circular islands each island contains a single-domain magnetic dipole below the Curie temperature $T_{C1} = 260\,\mathrm{K}$ of the $Pd_{0.87}Fe_{0.13}$ alloy. Below a second characteristic temperature T_{C2} at about 160 K, the pole interaction is strong enough to induce order in the form of interacting chains with increasing length at decreasing temperature. Simultaneously the increasing anisotropy yields an opening of the magnetic hysteresis with increasing coercivity and squareness. If the interaction of the islands on a square lattice were purely dipolar, such a situation would not occur. Instead a regular antiparallel array of canted chains and no magnetic hysteresis is expected. Thus, our present findings are hallmarks for higher pole interaction and, in particular, for a strong admixture of octopolar to the dipolar interaction as predicted by Monte Carlo simulations [2].

The authors are grateful to Peter Stauche and Jürgen Podschwadek for technical support in Bochum and Pascal Klamser for assistance at HZB. We would like to thank the Deutsche Forschungsgemeinschaft for financial support of this work within the SFB 491. The Helmholtz-Zentrum Berlin, including BESSY II, is supported by the BMBF.

*Present address: Jülich Centre for Neutron Science JCNS-2 and Peter Grünberg Institute PGI-4, Forschungszentrum Jülich GmbH, Jülich 52425, Germany.

[1] K. DeBell, A. B. MacIsaac, I. N. Booth, and J. P. Whitehead, Phys. Rev. B **55**, 15 108 (1997).
[2] E. Y. Vedmedenko, N. Mikuszeit, H. P. Oepen, and R. Wiesendanger, Phys. Rev. Lett. **95**, 207202 (2005).
[3] P. J. Jensen and G. M. Pastor, New J. Phys. **5**, 68 (2003).
[4] P. Politi and M. G. Pini, Phys. Rev. B **66**, 214414 (2002).
[5] R. L. Stamps and R. E. Camley, Phys. Rev. B **60**, 11 694 (1999).
[6] K. Yu. Guslienko, Appl. Phys. Lett. **75**, 394 (1999).
[7] E. Olive and P. Molho, Phys. Rev. B **58**, 9238 (1998).
[8] E. Y. Vedmedenko and N. Mikuszeit, ChemPhysChem **9**, 1222 (2008).
[9] C. A. Ross, M. Hwang, M. Shima, J. Y. Cheng, M. Farhoud, T. A. Savas, H. I. Smith, W. Schwarzacher, F. M. Ross, M. Redjdal, and F. B. Humphrey, Phys. Rev. B **65**, 144417 (2002).
[10] J. Y. Cheng, W. Jung, and C. A. Ross, Phys. Rev. B **70**, 064417 (2004).
[11] L. J. Heyderman, H. H. Solak, C. David, D. Atkinson, R. P. Cowburn, and F. Nolting, Appl. Phys. Lett. **85**, 4989 (2004).
[12] W. Kleemann, O. Petracic, Ch. Binek, G. N. Kakazei, Yu. G. Pogorelov, J. B. Sousa, S. Cardoso, and P. P. Freitas, Phys. Rev. B **63**, 134423 (2001).
[13] S. Prakash and C. L. Henley, Phys. Rev. B **42**, 6574 (1990).
[14] A. J. Bennett and J. M. Xu, Appl. Phys. Lett. **82**, 2503 (2003).
[15] R. F. Wang, C. Nisoli, R. S. Freitas, J. Li, W. McConville, B. J. Cooley, M. S. Lund, N. Samarth, C. Leighton, V. H. Crespi, and P. Schiffer, Nature (London) **439**, 303 (2006).
[16] J. P. Morgan, A. Stein, S. Langridge, and C. H. Marrows, Nat. Phys. **7**, 75 (2011).
[17] A. Remhof, A. Schumann, A. Westphalen, H. Zabel, N. Mikuszeit, E. Y. Vedmedenko, T. Last, and U. Kunze, Phys. Rev. B **77**, 134409 (2008).
[18] G. Möller and R. Moessner, Phys. Rev. Lett. **96**, 237202 (2006).
[19] J. A. Mydosh, J. I. Budnick, M. P. Kawatra, and S. Shlski, Phys. Rev. Lett. **21**, 1346 (1968).
[20] G. J. Nieuwenhuys, Adv. Phys. **24**, 515 (1975).
[21] M. Ewerlin, B. Pfau, C. Günther, S. Heinze, S. Eisebitt, R. Abrudan, and H. Zabel (unpublished).
[22] E. Dudzik, S. S. Dhesi, H. A. Dürr, S. P. Collins, M. D. Roper, G. van der Laan, K. Chesnel, M. Belakhovsky, A. Marty, and Y. Samson, Phys. Rev. B **62**, 5779 (2000).
[23] K. Chesnel, M. Belakhovsky, F. Livet, S. P. Collins, G. van der Laan, S. S. Dhesi, J. P. Attané, and A. Marty, Phys. Rev. B **66**, 172404 (2002).
[24] M. Donahue and D. Porter, http://math.nist.gov/oommf/.
[25] J. K. Ha, R. Hertel, and J. Kirschner, Phys. Rev. B **67**, 064418 (2003).
[26] P. Szary, O. Petracic, F. Brüssing, M. Ewerlin, and H. Zabel, J. Appl. Phys. **107**, 113922 (2010).
[27] F. Kronast, J. Schlichting, F. Radu, S. K. Mishra, T. Noll, and H. A. Dürr, Surf. Interface Anal. **42**, 1532 (2010).
[28] Y. B. Xu, A. Hirohata, S. M. Gardiner, M. Tselepi, J. Rothman, M. Kläui, L. Lopez-Diaz, J. A. C. Bland, Y. Chen, E. Cambril, and F. Rousseaux, IEEE Trans. Magn. **37**, 2055 (2001).